IEEE Access
Multidisciplinary | Rapid Review | Open Access Journal

Received 2 May 2023, accepted 22 May 2023, date of publication 29 May 2023, date of current version 7 June 2023.

Digital Object Identifier 10.1109/ACCESS.2023.3280564

RESEARCH ARTICLE

An Improved VME Technique via Heap Based Optimization Algorithm and AWIT Method for PLI and MA Noise Elimination in ECG

PAVAN G. MALGHAN AND MALAYA KUMAR HOTA
Department of Communication Engineering, School of Electronics Engineering, Vellore Institute of Technology, Vellore, Tamil Nadu 632014, India
Corresponding author: Malaya Kumar Hota (malayakumar.h@vit.ac.in)

ABSTRACT Diagnosing cardiac conditions require careful examination of an electrocardiogram (ECG). However, a significant issue arises when capturing an ECG due to interference from various noises. Noises like power line interference (PLI) and muscle artifact (MA) change the morphology, making it difficult to interpret the original signal. Our research proposes an improved variational mode extraction (IVME) technique using a Heap-based optimization (HBO) algorithm and an automatic wavelet interval-dependent thresholding (AWIT) method to eliminate such noises. First, HBO uses the envelope entropy spectrum (EES) as the objective function to find the best fitness value for optimizing the VME parameter, known as penalty factor α. Then, we extract a specific mode using the optimal α value in VME to accurately remove PLI from the signal. Finally, the AWIT method automatically computes the intervals and their respective threshold values to remove excessive MA noise from the PLI-filtered ECG signal. We evaluate the efficiency of ten random real-time ECG signals from the MIT-BIH arrhythmia database. The result analysis proves that our algorithm can accurately extract the mode containing PLI and eradicate MA from the noisy ECG signal. It also shows improvement in signal parameters like signal-to-noise ratio ($SNR_{improvement}$), mean square error (MSE), and correlation coefficients (CC) with 36.7968 dB, 0.00030901, and 99.7278%, respectively.

INDEX TERMS Automatic wavelet interval-dependent thresholding, electrocardiogram signal, envelope entropy spectrum, heap-based optimization algorithm, muscle artifact, power line interference, variational mode extraction.

I. INTRODUCTION

Electrocardiogram (ECG) signal is susceptible to artifacts and noises, which could contribute to signal distortion, affecting the morphological structure [1]. The noises such as electromyographic noise (EMG) or muscle artifact (MA), powerline interference (PLI), baseline wander/drift (BW), electrode motion noises (EM), and white Gaussian noise (WGN) alter the frequency information of the ECG signal. PLI and MA are the most prevalent artifacts interfering with ECG signal recording [2]. Due to patient movement during ECG recording, EMG or MA noise may reach 20% of a typical peak-to-peak ECG amplitude, whereas PLI has a frequency component at 50 Hz created by the power supply or AC source. Therefore, researchers have suggested novel approaches to remove these unwanted noises from ECG signals. Decomposition methods like empirical mode decomposition (EMD), ensemble EMD (EEMD), complete EEMD (CEEMD), variational mode decomposition (VMD), and variational mode extraction (VME) help to analyze and decompose the signals. However, these methods have their pros and cons for filtering the noise. EMD is a recursive technique that breakdowns a signal producing different frequency bands [3], [4], [5]. It causes a mode mixing problem. EEMD overcomes this problem by adding random white noise to an input signal [6], [7]. CEEMD can also address the mode mixing problem to some degree, but they introduce new complications, such as significant residual noise and spurious artifacts after decomposition [8], [9]. VMD is the non-recursive technique using a center frequency of the signal to retrieve constrained modes simultaneously [10], [12], [13]. Unlike VMD, VME extracts only one frequency

The associate editor coordinating the review of this manuscript and approving it for publication was Huaqing Li.

band and considers the spectral overlap and residual [14], [15]. It outperforms VMD in computation speed and precision. Before employing VME, two critical factors are necessary: the initial central frequency and the penalty factor. Also, a few filtering approaches, such as wavelet transforms, adaptive filtering, Kalman filtering, independent component analysis, and others, aid in noise elimination [16], [17], [18], [19], [20]. Combining these procedures contribute to the excellent interpretation of the ECG signal.

Various metaheuristic optimization algorithms were proposed in the past decade and evaluated on ECG data to optimize signal parameters. For example, optimization methods like particle swarm optimization (PSO) [21], grasshopper optimization algorithm (GOA) [22], and grey wolf optimization (GWO) [23], [24] are population-based metaheuristic optimization techniques relying on the collective behaviour of a group of agents to solve complex optimization problems. The main objective is to search for a global optimum. Nowadays, researchers use hybrid optimization algorithms combined with filtering techniques to deal with the drawback of individual algorithms to improve the efficiency and accuracy of the filtering process. For example, S. Balasubramanian et al. proposed a filtering method using an optimized adaptive hybrid filter and empirical wavelet transform using the Honey Badge optimization algorithm [25]. Zaid Abdi Alkareem Alyasseri et al. recommended a fusion method of β-hill climbing and wavelet transform to filter noisy ECG signals [26]. Agya Ram Verma et al. introduced evolutionary algorithms in constructing an adaptive noise canceller using PSO [27]. Narinder Singh and S. B. Singh suggested a hybrid PSO-GWO technique for improving convergence performance [28]. It overcame the limitations of both GWO and PSO and achieved optimal overall performance. Xinming Zhang et al. proposed a new hybrid algorithm (Hybrid GWO with PSO, HGWOP) for improved performance on complex functions and K-means clustering optimization [29].

Moreover, the researchers proved that combining the two techniques improves optimization productivity and leads to faster, more accurate, and more robust solutions. Over the past few decades, nature-inspired optimization algorithms have made many improvements. In addition, researchers have mapped natural processes and occurrences from all aspects of life on optimization methods. They are of four categories: evolution-based algorithms, swarm-based algorithms, physics-based algorithms, and human behaviour-based algorithms [30].

The results of human behaviour-based algorithms outperformed the other three groups [31]. As a consequence, we proposed an improved VME (IVME) technique based on a novel Heap-Based optimization algorithm (HBO), which is a human behaviour-based optimization algorithm along with an automatic wavelet interval-dependent thresholding (AWIT) for PLI and MA elimination in ECG. The HBO avoids local optima to obtain the best fitness value to optimize the VME parameter penalty factor (α). The proper selection of α is critical for efficiently removing PLI noise from an ECG signal. We use the minimum envelope entropy spectrum (EES) [32] as the objective function of HBO. In addition, the AWIT method helps to clean the corrupted ECG data from any lingering MA noise. Fig. 1 illustrates the two-stage filtering approach of our proposed method.

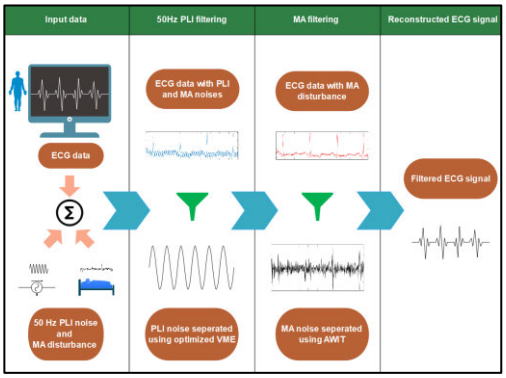

FIGURE 1. Two-stage filtering approach of our proposed method.

The HBO-based approach is easily adaptable to various ECG datasets. Furthermore, it is more accurate and flexible than existing methods, showing higher performance with a faster convergence curve. The VME extracts the specific frequency component containing PLI noise. On the other hand, the AWIT method can deal with different non-linear noises as it is difficult to eliminate using conventional filtering methods. Therefore, the AWIT algorithm helps in the better reduction of MA. As a result, combining HBO-based VME and AWIT is a significant step for noise removal with a two-stage filtering strategy. This article has the following sections: Section II explains our proposed technique, which utilizes an HBO algorithm and AWIT technique for VME parameter optimization to reduce PLI and MA noises; Section III describes the results found on the ECG signal parameters; Section IV discusses the algorithm's performance and efficiency with morphological outputs; and finally, section V concludes the work.

II. METHODOLOGY

Our proposed work addresses the application of the HBO-based IVME technique with the AWIT algorithm to denoise corrupted ECG data. The pseudo-code in Table 1 and the block diagram from Fig. 2 provide a brief idea of our proposed algorithm. This section contains three following sections; (A) ECG database and artifacts used for simulation, (B) proposed IVME Technique using HBO and (C) MA noise removal using AWIT algorithm.

A. ECG DATABASE AND ARTIFACTS USED FOR SIMULATION

The MIT-BIH arrhythmia database (mitdb) is a collection of 48 two-channel ECG signals from Beth Israel Hospital's laboratory in Boston [33]. Each contains data from 48 distinct individuals with approximately a half-hour duration.

Each signal has 650000 samples. About 60 per cent of the readings were from inpatients, while 40 per cent were from outpatients. Real-time signals were bandpass filtered and digitally captured at a 360 Hz sampling rate by the MIT Biomedical Engineering Centre. The overall length of each entry is 30 minutes and 5.556 seconds, but the sum may not precisely equal 30:06 due to a rounding mistake. The leads known as modified limb lead II (MLII) and lead V5, attaching chest electrodes, were frequently used to sense electrical impulses. We used those signals in our study because the MLII-based lead's features of QRS complexes were more prominent. We randomly selected ten ECG records of the first 1000 samples with a gain of 200 dB and added two types of noises. The first is PLI noise, which has a frequency of 50 Hz and a 15% peak amplitude value of a clean ECG signal. The second type of noise is the MA noise, which has a peak amplitude of 20%, a standard deviation equal to 0.15, and a mean of 0. This type of noise is generally random. As reflected in Fig. 3, our study used the ECG record '100' for simulation and a graphical representation.

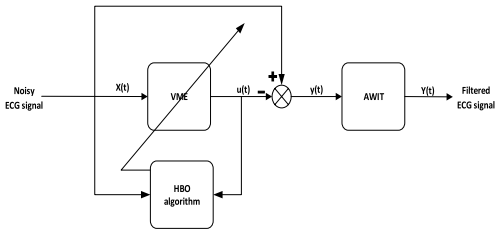

FIGURE 2. Block diagram of the proposed algorithm.

TABLE 1. Pseudo-code of the proposed algorithm.

1.	Load ECG data: x(t).
2.	Add PLI noise ($n_1(t)$) and MA noise ($n_2(t)$) to x(t) to get X(t).
3.	Set the initial parameters of HBO: lb, ub, dim, fobj, noP, maxIter.
4.	Initialize the VME parameter by setting the range of α.
5.	Perform HBO for 'maxIter' iterations.
6.	Decompose the signal X(t) into VMF at each iteration.
7.	Find the fitness values of all VMFs and store the best fitness values.
8.	Store the best global fitness value.
9.	Re-run VME with updated fitness value to decompose X(t) into a new VMF u(t).
10.	Eliminate u(t) from X(t) to get a PLI-filtered signal, y(t).
11.	Apply the 2-level AWIT on y(t) to detect the intervals and thresholding parameters.
12.	Apply the threshold values for each interval to filter MA noise, $n_2(t)$.
13.	Reconstruct the signal to get a filtered ECG signal: Y(t).

B. PROPOSED IVME TECHNIQUE USING HBO

The HBO algorithm is a mathematical approach to determining the best solution for a problem based on a given set of criteria. It uses a heap data structure to store the pairs of

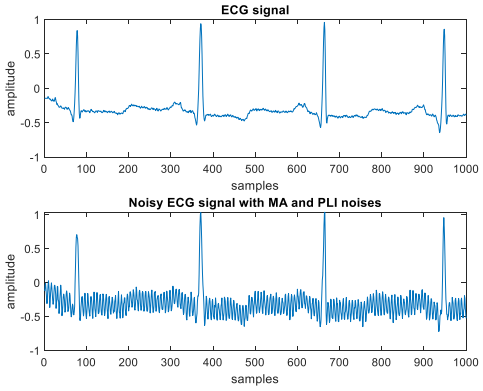

FIGURE 3. Input ECG record '100' with PLI and MA noises.

criteria and associated values, with the best possible solution being determined by a given minimum value of each criterion.

Fig. 4 shows a triangular framework to simulate a minimum heap data structure. We can see that each person has only one direct boss on the level above them, but all people on the same level are their co-workers. For example, node H_5 only has one direct boss, H_2, but its colleague H_7 is on the same hierarchy level. Likewise, H_4 is the direct boss of both H_2 and H_6. It is the same for all the other nodes in the system if there are any.

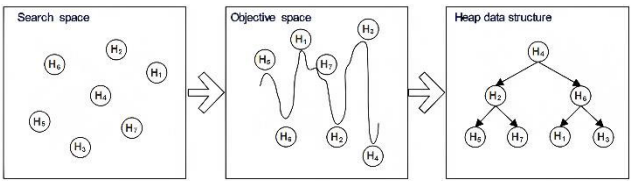

FIGURE 4. Organization chart (OC) with a minimum heap structure.

OC represents the search space in the HBO algorithm. The process begins by examining the rank hierarchy and considering the criteria for identifying the optimal structure. It primarily requires three aspects: the interaction between the co-workers and their immediate leader, the interaction between the individual and their co-workers, and the individual's self-contribution [30]. HBO can be applied to a corporate rank hierarchy to maximize efficiency. Table 2 explains the HBO algorithm with pseudo-code [31]. Here t is the current iteration number, T is the total number of iterations, j is the dimension's position, j [1, D], D is the dimension of a search space, i is the measure of an individual, i [1, N] is the count in the population, N is the population size, p is random number distributed uniformly in (0, 1) with p_1 and p_2 as probabilities values with Eq. (1) and Eq. (2) as follows:

$$p_1 = 1 - \frac{t}{T} \tag{1}$$

$$p_2 = p_1 + \frac{1 - p_1}{2} \tag{2}$$

The mathematical equations for calculating the updated positions of all three aspects are in Eq. (3), Eq. (4), and

TABLE 2. Pseudo-code of the HBO algorithm.

```
Initialize the variables and randomly generate the population.
Compute the fitness of each individual and find the optimal solution.
Construct a priority heap.
for t=1: T
  for i=N: 2
    for j=1: D
if p ≤ p1
Execute the self-contribution update position equation as shown in Eq. (3).
  else if p > p1 and p ≤ p2
Update the position for interaction with the direct boss using Eq. (3).
  else
    if p > p2 and p ≤ 1
Update the position for interaction with the co-worker using Eq. (3).
    end if
end if
  end for
Bound the new position of the n^th individual.
Calculate the fitness of the n^th individual.
Update the individual and the optimal solution using a greedy strategy.
Refresh the heap.
  end for
end for
Store the optimal results.
```

Eq. (5) [31]. Compared to traditional optimization algorithms, HBO can identify the best solution quickly and accurately. Moreover, it enhances the performance of a hierarchical structure for a given search space. HBO has a more significant global optimization capacity than PSO, GWO, and HGWO. The primary distinction between these methods is that HBO uses the minimum heap data structure by mapping the OC concept in the optimization procedure. Table 3 shows the initial values for HBO parameters to optimize VME parameter α.

$$X_i^j(t+1) = \begin{cases} X_i^j(t), & p \le p_1 \\ B^j + \gamma\lambda^j \left| B^j - X_i^j(t) \right|, & p > p_1 \wedge p \le p_2 \\ S_r^j + \gamma\lambda^j \left| S_r^j - X_i^j(t) \right|, & p > p_2 \wedge p \le 1 \\ & \wedge f(S_r) \ge f(X_i(t)) \\ X_i^j + \gamma\lambda^j \left| S_r^j - X_i^j(t) \right|, & p > p_2 \wedge p \le 1 \\ & \wedge f(S_r) < f(X_i(t)) \end{cases} \tag{3}$$

$$\gamma = \left| 2 - \left(\frac{t \times mod(\frac{T}{C})}{\frac{T}{4C}} \right) \right| \tag{4}$$

$$\lambda^j = 2r - 1 \tag{5}$$

X_i represents the worker's i^{th} position, and the direct boss and co-worker are represented by positions B and S, respectively. The scaling factor γ from Eq. (4) value ranges from (0, 2) depending on the repetition count. λ^j is a randomly generated vector where $\boldsymbol{r}$ is the random number same as p, as seen in Eq. (5), C is the user-defined parameter to fix the count of cycles in T iterations, and f is the fitness function used to calculate individual fitness value for a new location. For instance, if $f(S_r) \ge f(X_i(t))$, the worker can investigate the area around S_r, and if $f(S_r) < f(X_i(t))$, it permits exploration of the region around X_i. The present worker generates a new location by updating the position using Eq. (3) updating strategy.

TABLE 3. HBO initialization for VME optimization.

Input parameters	Value/range
lb	1000
ub	10000
dim	1
fobj	min (EES)
noP	50
maxIter	100
ω	50
τ	0
runs	25
ε	$1e^{-7}$

'*lb*' and '*ub*' denote the lower and upper bounds, '*dim*' represents the dimension of the space, and '*fobj*' is our objective function of HBO. '*noP*' is the total population size, '*maxIter*' denotes how many iterations to carry out, and 'τ' is the update parameter. Fig. 5 explains the detailed flowchart of our proposed algorithm.

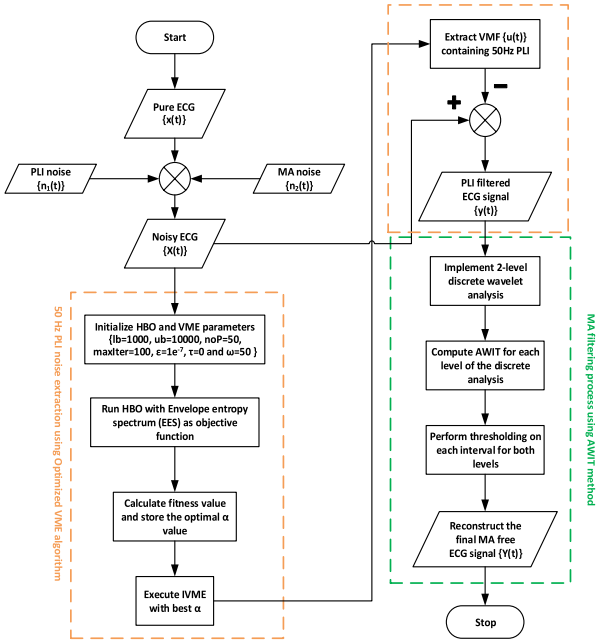

FIGURE 5. Proposed flowchart for ECG denoising.

The first step is to consider a clean ECG signal $x\,(t)$ added with PLI noise $n_1\,(t)$ and MA noise $n_2\,(t)$ as given in Eq. (6):

$$X\,(t) = x\,(t) + n_1\,(t) + n_2\,(t) \tag{6}$$

Here, $X\,(t)$ is the noisy signal for filtering. We perform a comparative simulation between HBO and three other optimization techniques. The main aim is to evaluate the efficacy of the IVME in parameter tuning. As stated in Eq. (9), the EES is the objective function used for our research. Using Eq. (7) and Eq. (8), we obtain EES by calculating the envelope of $X\,(t)$ and performing the fast Fourier transform (FFT) on $e(t)$.

$$e\,(t) = \sqrt{X(t)^2 + H\{X\,(t)\}^2} \tag{7}$$

$$E_i(t) = |FFT\{e(t)\}| \tag{8}$$

$$EES = -\sum_{i=1}^{n} E_i \log_2 E_i \tag{9}$$

Here, H represents Hilbert transform, and E_i is the envelope spectrum of $X\,(t)$.

A minimum EES value is considered the best fitness value of the HBO algorithm to optimize α. Therefore, we choose a limit of 100 iterations for these algorithms and with 50 search agents. Fig. 6 depicts the comparison outcome. HBO converges to the best fitness score for EES in a few iterations, precisely at the 9th iteration, whereas PSO, GWO, and HGWO require 59, 99, and 96 iterations, respectively.

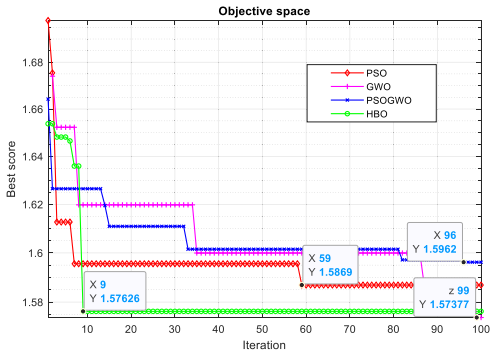

FIGURE 6. Convergence curves of PSO, GWO, HGWO, and HBO algorithms.

TABLE 4. VME algorithm.

1. Initialize $\hat{u}_s^1$, λ^1, i $\leftarrow$ 0 and ω_s^1 (initial assumption)
2. Repeat for i $\leftarrow$ i + 1
3. Update $\hat{\omega}_s$ for all $\omega \geq 0$:
   $\hat{u}_s^{i+1} = \frac{\hat{f}(\omega)+\alpha^2(\omega-\omega_s^{i+1})^4\hat{u}_s^i(\omega)+\frac{\hat{\lambda}(\omega)}{2}}{[1+\alpha^2(\omega-\omega_s^{i+1})^4][1+2\alpha(\omega-\omega_s^i)^2]}$
4. Update ω_s:
   $\omega_s^{i+1} = \frac{\int_0^\infty \omega\left|\hat{u}_s^{i+1}(\omega)\right|^2 d\omega}{\int_0^\infty \left|\hat{u}_s^{i+1}(\omega)\right|^2 d\omega}$
5. Dual ascent for all $\omega \geq 0$:
   $\hat{\lambda}^{i+1} = \hat{\lambda}^i + \tau\left[\frac{\hat{f}(\omega)+\hat{u}_s^{i+1}(\omega)}{1+\alpha^2(\omega-\omega_s^{i+1})^4}\right]$
6. Until convergence: $\frac{\left\|\hat{u}_s^{i+1}-\hat{u}_s^i\right\|_2^2}{\left\|\hat{u}_s^i\right\|_2^2} < \varepsilon$

HBO helps the VME to achieve the best value for α with a fast convergence curve, as Fig. 6 shows the HBO algorithm outperforming other optimization methods. Furthermore, compared to PSO and HGWO, HBO has a reduced EES value of 1.57626. The HBO algorithm outperforms the other three optimization methods concerning fast convergence rate. The best value of α obtained using the preceding method is 1637.3002. We use this value to execute the IVME algorithm as given in Table 4 to extract PLI present in a specific mode $u\,(t)$. However, there is still excessive noise in PLI-filtered ECG signal $y\,(t)$. Therefore, we use the AWIT technique to filter out the residual noise.

C. MA NOISE REMOVAL USING AWIT ALGORITHM

DWT transform is a method that uses multiresolution filter banks like low and high-pass filters with specified mother wavelets. The most common types of DWT filtering are single-stage and multi-stage DWT. The filtering technique divided the input signal into the low-pass and high-pass components with downsampling, yielding approximation (A1 and A2) and detail (D1 and D2) coefficients. A multi-stage DWT method lets us choose the decomposition stages to obtain multiple frequency bands. As depicted in Fig. 7, our work implements a two-stage wavelet decomposition analysis for the noisy signal to filter out the MA noise at the last stage efficiently. The wavelet interval thresholding method is a filtering process where the filter here is a wavelet, an oscillatory signal modified for a precise application. The filtering process involves dividing a signal to obtain frequency components, also known as intervals. Interval thresholding is setting a minimum and maximum value for the signal to determine whether it falls within a specified range [34]. Eq. (10) gives the formula for interval thresholding:

$$F\,(x) = \begin{cases} 1, & if\ x > t_1 \wedge x \leq t_2 \\ 0, & otherwise \end{cases} \tag{10}$$

x is the input data for testing; the lower and upper threshold values are t_1 and t_2, respectively, and the output is the binary value 1 or 0.

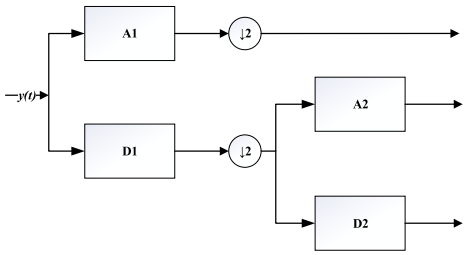

FIGURE 7. A two-stage wavelet decomposition to filter MA noise.

But in the case of AWIT, it is an automated process that detects and removes noise from signals without requiring the user to determine whether to keep or discard the components manually. This process is beneficial in signal and image processing applications, where the manual selection

of components is often time-consuming and error-prone. Table 5 thoroughly explains the pseudo-code of the AWIT technique [35]. AWIT automatically calculates the intervals and the thresholds for all the detected intervals rather than manually setting them. Finally, the process concludes by performing the thresholding process for each interval detected with their specific threshold values to remove excess noise, then reconstructing and illustrating the final signal.

TABLE 5. Pseudo-code of the AWIT algorithm.

1.	Obtain the coefficient values and coefficient vector length.
2.	Compute the maximum values of the coefficient vector.
3.	Set the maximum intervals to 6.
4.	If the intervals are not available, set it to 'NaN.'
5.	Extract the detail of order 1.
6.	Compute the x values of the input vector.
7.	Replace 2 per cent of the input vector's highest values by mean and find breaking points.
8.	Compute the optimal number of intervals
9.	If no intervals are present, set it to 'nb_Opt_Int.'
10.	Apply the denoising structure.
11.	Compute intervals and de-thresholding parameters for each interval.
12.	Create two cells to store 'int_DepThr' and the optimal interim
13.	Store optimal interim intervals and compute threshold values.
14.	Output the cells' thrParams' and 'int_DepThr_Cell.'

In our work, after removing the 50 Hz PLI noise from the noisy ECG signal $X(t)$ using IVME, the signal $y(t)$ undergoes wavelet thresholding to decompose the signals into wavelet coefficients. Then, the AWIT algorithm automatically computes the intervals in each coefficient. First, it calculates the t_1 and t_2 values using Eq. (10) depending on the length of the ECG signal. Then, replacing two per cent of the highest values of input vectors with the mean, AWIT automatically finds the breakpoints in each interval, as Table 5 mentions. Finally, it computes the threshold values for every interval obtained to execute the soft thresholding of coefficients. We reconstruct the signal using the wavelet coefficients A1, A2, and D2 to obtain a noise-free ECG signal $Y(t)$.

III. RESULTS

This section demonstrates a thorough simulation to assess our proposed technique for the ECG filtering process by tabulating the results. We performed all the simulations on a recent MATLAB 2022a software. We use ten randomly selected real-time ECG signals from the MIT-BIH arrhythmia database (ECG records: 100, 102, 105, 111, 115, 118, 205, 213, 220, and 230) at a sampling frequency of 360 Hz and 200 dB gain. We estimate the ECG signal quality at the output using the performance metrics such as signal-to-noise ratio (SNR), mean square error (MSE), and correlation coefficient (CC). To visually analyze the proposed research's efficacy, we take an ECG record '100' by limiting it to 1000 samples for the study. The mathematical formulae for these performance metrics are as below:

$$SNR_{in} = 10log_{10}\frac{\sum_{n=1}^{N}[x(n)]^2}{\sum_{n=1}^{N}[X(n)-x(n)]^2} \tag{11}$$

$$SNR_{out} = 10log_{10}\frac{\sum_{n=1}^{N}[x(n)]^2}{\sum_{n=1}^{N}[Y(n)-x(n)]^2} \tag{12}$$

$$SNR_{improvement} = SNR_{out} - SNR_{in} \tag{13}$$

$$MSE = \frac{1}{N}\sum_{n=1}^{N}[e(n)-y(n)]^2 \tag{14}$$

$$CC = \frac{\sum_{n=1}^{N}(x(n)-\bar{x}(n))(Y(n)-\bar{Y}(n))}{\sqrt{\sum_{n=1}^{N}(x(n)-\bar{x}(n))^2}\sqrt{\sum_{n=1}^{N}(Y(n)-\bar{Y}(n))^2}} \tag{15}$$

N denotes the total samples, $x(n)$ is a clean ECG signal, $X(n)$ is the noisy signal contaminated with PLI and MA noise, $Y(n)$ is the filtered output, $\bar{x}(n)$, and $\bar{Y}(n)$ are the means of clean and filtered signals, respectively. Tables 6, 7, and 8 show the simulated performance metrics regarding SNR, MSE, and CC, proving that our technique efficiently removes both noises. Table 6 shows SNR improvement results and the optimal fitness values obtained using the HBO algorithm. ECG record '105' has the best fitness value of 1.1761, giving an optimal α value of 1775.4642. We had set the initial range of α to [1000, 10000] for parameter optimization of the VME algorithm. HBO provides the best value compared to PSO and the other two algorithms due to the fast convergence criterion. Using the optimal α value, we calculated the signal parameters of the filtered ECG after performing VME, VME-Single value Thresholding (VME-ST), and our proposed method. As a result, we obtained significant improvement in SNR with 36.7968 dB on an average of ten random ECG signals. Furthermore, from Table 7 and Table 8, MSE and CC results with a value of 0.00030901 and 99.7278% show a better performance in filtering PLI and MA noises.

IV. DISCUSSION

Before evaluating the currently available approaches, we use the EMD approach to decompose the noisy signal $X(t)$ into intrinsic mode functions (IMFs). The mode mixing impact is the main disadvantage of EMD. When multiple oscillations of different time scales mix in a single frequency band or when assigning oscillations of the same time scale to different IMFs, we say that there is mode mixing. The EEMD and CEEMD techniques came into existence to counteract this, which involve gradually adding white noise to the signal to cancel out the mode-mixing impact. The ECG data were filtered using a combination of SWT and those other techniques. In addition to the two techniques in Table 9, we also

TABLE 6. Improvement in SNR for ten ECG signals from the 'MITDB' database.

ECG RECORD	Optimal EES value	Optimal α value	SNR_{in} (dB)	SNR_{out} (dB)			$SNR_{improvement}$ (dB)		
				VME	VME-ST	Proposed method	VME	VME-ST	Proposed method
100	1.5763	1637.3002	24.3985	51.4402	55.9812	**58.1445**	27.0417	31.5827	**33.7459**
102	1.6914	8672.5829	17.9675	37.9394	47.8221	**49.8935**	19.9719	29.8546	**31.9261**
105	1.1761	1775.4642	26.43	64.1566	66.2558	**66.9598**	37.7266	39.8258	**40.5297**
111	1.5811	10000	14.3198	48.869	51.93	**52.3479**	34.5493	37.6102	**38.0281**
115	1.1858	5870.4847	33.5137	55.1108	68.6968	**73.7013**	21.5971	35.1831	**40.1876**
118	1.7108	9065.28	46.1343	67.9237	75.5881	**78.9916**	21.7894	29.4537	**32.8573**
205	1.2712	3034.2868	28.8048	63.4431	64.8927	**70.7228**	34.6383	36.0879	**41.918**
213	1.2248	3043.1329	36.928	65.0023	71.3594	**72.6103**	28.0743	34.4314	**35.6823**
220	1.3069	2570.5062	38.0673	53.8721	69.19	**71.3533**	15.8048	31.1227	**33.286**
230	1.274	9881.3708	29.1911	57.924	64.3056	**68.998**	28.733	35.1146	**39.807**
Average	**1.2726**	**5050.0372**	**26.8868**	**56.5681**	**63.6022**	**66.3723**	**26.9926**	34.0267	***36.7968***

TABLE 7. MSE estimation of ten random ECG signals.

ECG RECORD	MSE		
	VME	VME-ST	Proposed method
100	0.00076345	0.00048481	**0.0003905**
102	0.0015646	0.00058238	**0.00047341**
105	0.00026643	0.00021598	**0.0002013**
111	0.00036175	0.00026636	**0.00025546**
115	0.0013368	0.00034358	**0.0002083**
118	0.0013089	0.0006082	**0.00043275**
205	0.00036238	0.00031348	**0.00017499**
213	0.00069717	0.00036919	**0.00032578**
220	0.0023677	0.00051177	**0.00041221**
230	0.00065174	0.00034429	**0.00021535**
Average	**0.00096809**	**0.000404**	***0.00030901***

TABLE 8. MSE estimation of ten random ECG signals.

ECG RECORD	CC (%)		
	VME	VME-ST	Proposed method
100	98.8571	99.2769	**99.4177**
102	97.6541	99.1399	**99.2963**
105	99.8526	99.8805	**99.8886**
111	99.3613	99.5276	**99.5469**
115	99.2496	99.808	**99.8834**
118	99.5257	99.7798	**99.8439**
205	99.4416	99.5227	**99.7309**
213	99.8926	99.9432	**99.9499**
220	98.9203	99.7676	**99.8134**
230	99.7184	99.8516	**99.9071**
Average	**99.2473**	**99.6498**	***99.7278***

compared the CEEMD-SWT method. When comparing the final filtered outputs from EMD-SWT, EEMD-SWT, and CEEMD-SWT, it successfully filters out high-frequency PLI noise and maintains the QRS peak, but it cannot filter out the MA noise effectively. To effectively eliminate noisy data, the NLM filtering approach helped many researchers. These methods effectively reduce MA noise. However, data loss is a significant problem. After processing, the R-peak information in the ECG signal is not up to the mark.

Signal decomposition in the VMD-DWT technique, which is superior to the EMD-based method, needs fixed K and α. The decision of which values to use is purely experimental. Randomly picking values is never a good idea. To overcome the shortcoming, optimization methods like PSO, GOA, GWO, and HBO are put into place to determine the best possible numbers of K and α.

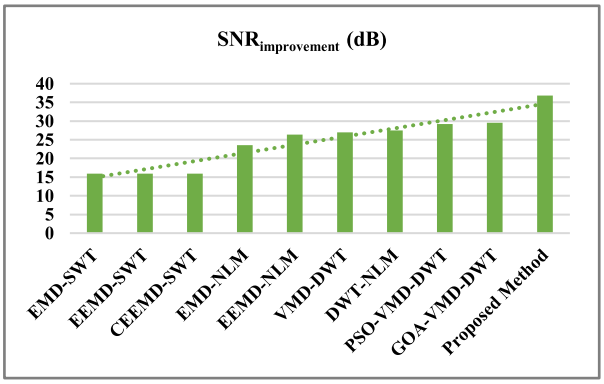

FIGURE 8. $SNR_{improvement}$ chart of all methods.

While the flexibility of VMD approaches based on intelligent algorithms is high, their poor operational efficiency

TABLE 9. Comparison of the proposed algorithm with existing methods.

Algorithms	$SNR_{improvent}$ (dB)	MSE	CC (%)
EMD-SWT [36]	15.9241	1.3405	95.3985
EEMD-SWT [36]	15.9092	1.3343	95.6149
CEEMD-SWT	15.9024	1.3319	95.5935
EMD-NLM [37]	23.5338	0.0056598	96.9017
EEMD-NLM [37]	26.4173	0.0098004	97.5780
VMD-DWT [38]	26.9941	0.016032	97.8045
DWT-NLM [37]	27.459	0.01095	97.8228
PSO-VMD-DWT [22]	29.2179	0.0080468	98.1811
GOA-VMD-DWT [22]	29.5249	0.0080787	98.2363
Proposed Method	**36.7968**	**0.00030901**	**99.7278**

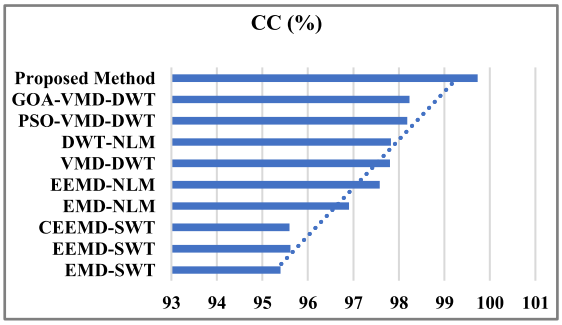

FIGURE 9. CC chart of all methods.

severely limits their use for filtering particular noise. VME is a cutting-edge filtration method that efficiently separates a narrow-band mode from a signal with multiple components. Therefore, we use this strategy with HBO to quickly identify the α. DWT thresholding is a standard method for signal filtering and smoothing. However, the requirement of thresholding values is also mandatory. The AWIT method overcomes this requirement problem and effectively filters out unwanted noises by automatically finding intervals and their respective threshold values.

The proposed technique is compared with various filtering methods such as EMD-SWT [36], EEMD-SWT [36], EMD-NLM [37], EEMD-NLM [37], DWT-NLM [37], VMD-DWT [38], PSO-VMD-DWT [22], and GOA-VMD-DWT [22] to validate its denoising capabilities. Fig. 8 and Fig. 9 represent bar charts of the improvement in SNR and CC parameters. Table 9 shows the significant results of all ten ECG record's average values. Compared to all the filtering approaches, our suggested methodology has the best SNR, MSE, and CC values of 36.7968 dB, 0.00030901, and 99.7278%, respectively. Fig. 10 shows the graphical representation of the ECG record '100' after removing 50 Hz PLI noise $n_1(t)$ with the help of HBO and VME algorithms. However, MA noise $n_2(t)$ remains in the output signal obtained after the VME process. Therefore, wavelet thresholding is a must for removing excess noise. Finally, we compare the

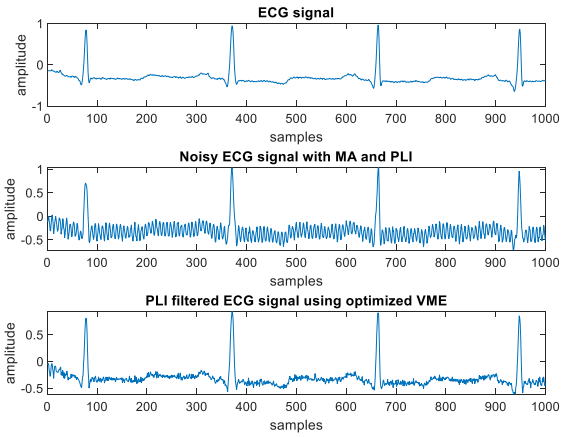

FIGURE 10. ECG signal after 50 Hz PLI removal using the IVME method.

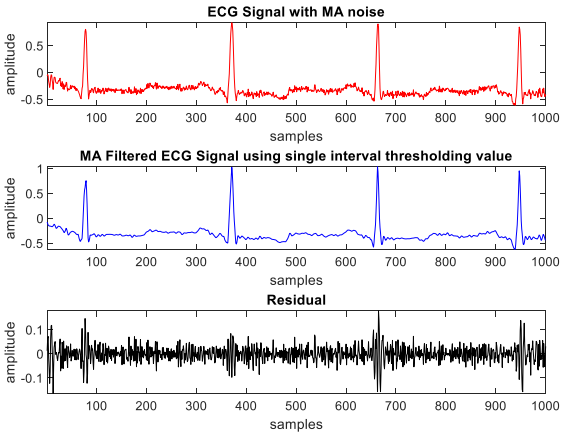

FIGURE 11. ECG signal after MA removal using the VME-ST method.

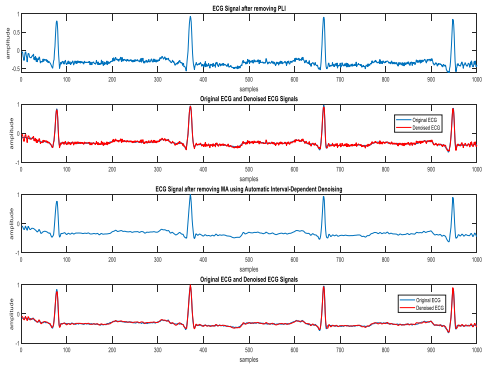

FIGURE 12. ECG signal after MA removal using the proposed method.

AWIT method with the traditional ST algorithm, as depicted in Fig. 11 and Fig. 12. A residual after performing ST contains the MA noise. Although the ST method removes the MA noise, it cannot wholly denoise the signal due to noisy components at different intervals.

Hence, AWIT is the best method to decompose the signal $y(t)$ into relevant frequency components using a two-level wavelet decomposition. First, we feed the noisy signal to the AWIT algorithm to automatically compute intervals

containing noise and their particular threshold values. We use 'sym4,' the mother wavelet, for the wavelet denoising process, as it plays a crucial role and completely resembles the QRS peak in an ECG signal. We then apply soft thresholding to each interval with computed threshold values. Finally, from Fig. 12, we observe that the MA noise gets eliminated efficiently by choosing the appropriate wavelet coefficients for reconstructing the signal $Y(t)$.

V. CONCLUSION

This research article proposed an improved VME technique for ECG signal denoising by combining the heap-based optimizer with the automatic wavelet interval-dependent thresholding technique. The method accurately estimated the optimal penalty factor α for the VME algorithm to extract PLI noise from the corrupted ECG signal. The envelope entropy spectrum as an objective function for the HBO optimization proved to have a fast convergence speed compared to PSO, GWO, and HGWO. Furthermore, AWIT helped to eliminate MA noise from the ECG data with greater efficiency leading to improved signal quality in terms of SNR, MSE, and CC. The results showed that our proposed method outperformed all existing algorithms. Our method may be effective for ECG signal denoising applications in cardiac health monitoring devices and help the physician or a doctor to diagnose the arrhythmias flawlessly.

REFERENCES

[1] S. K. Berkaya, A. K. Uysal, E. S. Gunal, S. Ergin, S. Gunal, and M. B. Gulmezoglu, "A survey on ECG analysis," *Biomed. Signal Process. Control*, vol. 43, pp. 216–235, May 2018.

[2] U. Satija, B. Ramkumar, and M. S. Manikandan, "Automated ECG noise detection and classification system for unsupervised healthcare monitoring," *IEEE J. Biomed. Health Informat.*, vol. 22, no. 3, pp. 722–732, May 2018.

[3] M. Rakshit and S. Das, "An efficient ECG denoising methodology using empirical mode decomposition and adaptive switching mean filter," *Biomed. Signal Process. Control*, vol. 40, pp. 140–148, Feb. 2018.

[4] S. A. Malik, S. A. Parah, and B. A. Malik, "Power line noise and baseline wander removal from ECG signals using empirical mode decomposition and lifting wavelet transform technique," *Health Technol.*, vol. 12, no. 4, pp. 745–756, Jul. 2022.

[5] Y. Zhou, B. W. Ling, X. Mo, Y. Guo, and Z. Tian, "Empirical mode decomposition-based hierarchical multiresolution analysis for suppressing noise," *IEEE Trans. Instrum. Meas.*, vol. 69, no. 4, pp. 1833–1845, Apr. 2020.

[6] Z. Huang and B. W. K. Ling, "Joint ensemble empirical mode decomposition and tunable Q factor wavelet transform based sleep stage classifications," *Biomed. Signal Process. Control*, vol. 77, Aug. 2022, Art. no. 103760.

[7] A. S. Narla, S. Kapuganti, and H. Nenavath, "Noise removal in ECG signals utilizing fully convolutional DAE," in *Proc. Int. Conf. Comput. Intell.* Singapore: Springer, 2022, pp. 243–256.

[8] S. Sarkar, S. Bhattacherjee, P. Bhattacharyya, M. Mitra, and S. Pal, "Automatic identification of asthma from ECG derived respiration using complete ensemble empirical mode decomposition with adaptive noise and principal component analysis," *Biomed. Signal Process. Control*, vol. 77, Aug. 2022, Art. no. 103716.

[9] Z. Shamaee and M. Mivehchy, "Dominant noise-aided EMD (DEMD): Extending empirical mode decomposition for noise reduction by incorporating dominant noise and deep classification," *Biomed. Signal Process. Control*, vol. 80, Feb. 2023, Art. no. 104218.

[10] C. Li, Y. Wu, H. Lin, J. Li, F. Zhang, and Y. Yang, "ECG denoising method based on an improved VMD algorithm," *IEEE Sensors J.*, vol. 22, no. 23, pp. 22725–22733, Dec. 2022.

[11] B. Shanmukh and R. Shanmughasundaram, "Feature extraction of ECG signal using variational mode decomposition," in *Evolution in Signal Processing and Telecommunication Networks*, vol. 2. Singapore: Springer, 2022.

[12] H. Cao and L. Peyrodie, "Variational mode decomposition-based simultaneous r peak detection and noise suppression for automatic ECG analysis," *IEEE Sensors J.*, vol. 23, no. 8, pp. 8703–8713, Apr. 2023.

[13] X. Hu, Q. Yu, and H. Yu, "An ECG denoising method combining variational modal decomposition and wavelet soft threshold," *Concurrency Comput., Pract. Exper.*, p. e7048, 2022, doi: 10.1002/cpe.7048.

[14] M. Nazari and S. M. Sakhaei, "Variational mode extraction: A new efficient method to derive respiratory signals from ECG," *IEEE J. Biomed. Health Informat.*, vol. 22, no. 4, pp. 1059–1067, Jul. 2018.

[15] M. Shahbakhti, M. Beiramvand, M. Nazari, A. Broniec-Wójcik, P. Augustyniak, A. S. Rodrigues, M. Wierzchon, and V. Marozas, "VME-DWT: An efficient algorithm for detection and elimination of eye blink from short segments of single EEG channel," *IEEE Trans. Neural Syst. Rehabil. Eng.*, vol. 29, pp. 408–417, 2021.

[16] Z. Wang, J. Zhu, T. Yan, and L. Yang, "A new modified wavelet-based ECG denoising," *Comput. Assist. Surgery*, vol. 24, pp. 174–183, Oct. 2019.

[17] W. Jenkal, R. Latif, A. Toumanari, A. Dliou, O. El B'charri, and F. M. R. Maoulainine, "An efficient algorithm of ECG signal denoising using the adaptive dual threshold filter and the discrete wavelet transform," *Biocybernetics Biomed. Eng.*, vol. 36, no. 3, pp. 499–508, 2016.

[18] N. H. Beni and N. Jiang, "Heartbeat detection from single-lead ECG contaminated with simulated EMG at different intensity levels: A comparative study," *Biomed. Signal Process. Control*, vol. 83, May 2023, Art. no. 104612.

[19] J. D. K. Abel, S. Dhanalakshmi, and R. Kumar, "A comprehensive survey on signal processing and machine learning techniques for non-invasive fetal ECG extraction," *Multimedia Tools Appl.*, vol. 82, no. 1, pp. 1373–1400, Jan. 2023.

[20] S. Chatterjee, R. S. Thakur, R. N. Yadav, and L. Gupta, "Sparsity-based modified wavelet de-noising autoencoder for ECG signals," *Signal Process.*, vol. 198, Sep. 2022, Art. no. 108605.

[21] S. Jain, V. Bajaj, and A. Kumar, "Effective de-noising of ECG by optimised adaptive thresholding on noisy modes," *IET Sci., Meas. Technol.*, vol. 12, no. 5, pp. 640–644, Aug. 2018.

[22] P. G. Malghan and M. K. Hota, "Grasshopper optimization algorithm based improved variational mode decomposition technique for muscle artifact removal in ECG using dynamic time warping," *Biomed. Signal Process. Control*, vol. 73, Mar. 2022, Art. no. 103437.

[23] A. R. Verma and B. Gupta, "A novel approach adaptive filtering method for electromyogram signal using Gray Wolf optimization algorithm," *SN Appl. Sci.*, vol. 2, p. 16, Jan. 2020.

[24] S. R. Ramson, K. L. Raju, S. Vishnu, and T. Anagnostopoulos, "Nature inspired optimization techniques for image processing—A short review," in *Nature Inspired Optimization Techniques for Image Processing Applications* (Intelligent Systems Reference Library), vol. 150, J. Hemanth and V. Balas, Eds. Cham, Switzerland: Springer, 2019, doi: 10.1007/978-3-319-96002-9_5.

[25] S. Balasubramanian, M. S. Naruk, and G. Tewari, "Electrocardiogram signal denoising using optimized adaptive hybrid filter with empirical wavelet transform," *J. Shanghai Jiaotong Univ., Sci.*, 2023, doi: 10.1007/s12204-023-2591-1.

[26] Z. A. Alkareem Alyasseri, A. T. Khader, M. A. Al-Betar, and L. M. Abualigah, "ECG signal denoising using β-hill climbing algorithm and wavelet transform," in *Proc. 8th Int. Conf. Inf. Technol. (ICIT)*, May 2017, pp. 96–101.

[27] A. R. Verma, Y. Singh, and V. Joshi, "Adaptive filtering using PSO, MPSO and ABC algorithms for ECG signal," *Int. J. Biomed. Eng. Technol.*, vol. 21, no. 4, pp. 379–392, 2016.

[28] N. Singh and S. B. Singh, "Hybrid algorithm of particle swarm optimization and grey wolf optimizer for improving convergence performance," *J. Appl. Math.*, vol. 2017, pp. 1–15, Jan. 2017.

[29] X. Zhang, Q. Lin, W. Mao, S. Liu, Z. Dou, and G. Liu, "Hybrid particle swarm and grey wolf optimizer and its application to clustering optimization," *Appl. Soft Comput.*, vol. 101, Mar. 2021, Art. no. 107061.

[30] Q. Askari, M. Saeed, and I. Younas, "Heap-based optimizer inspired by corporate rank hierarchy for global optimization," *Exp. Syst. Appl.*, vol. 161, Dec. 2020, Art. no. 113702.

[31] X. Zhang and S. Wen, "Heap-based optimizer based on three new updating strategies," *Exp. Syst. Appl.*, vol. 209, Dec. 2022, Art. no. 118222.

[32] J. Sun, Q. Xiao, J. Wen, and F. Wang, "Natural gas pipeline small leakage feature extraction and recognition based on LMD envelope spectrum entropy and SVM," *Measurement*, vol. 55, pp. 434–443, Sep. 2014.
[33] G. B. Moody and R. G. Mark, "The impact of the MIT-BIH arrhythmia database," *IEEE Eng. Med. Biol. Mag.*, vol. 20, no. 3, pp. 45–50, May/Jun. 2001.
[34] G. Yang, Y. Liu, Y. Wang, and Z. Zhu, "EMD interval thresholding denoising based on similarity measure to select relevant modes," *Signal Process.*, vol. 109, pp. 95–109, Apr. 2015.
[35] T. MathWorks. *Wavelet Toolbox Documentation*. Accessed: Feb. 24, 2023. [Online]. Available: https://in.mathworks.com/help/wavelet/ug/wavelet-interval-dependent-denoising.html
[36] A. K. Dwivedi, H. Ranjan, A. Menon, and P. Periasamy, "Noise reduction in ECG signal using combined ensemble empirical mode decomposition method with stationary wavelet transform," *Circuits, Syst., Signal Process.*, vol. 40, no. 2, pp. 827–844, Feb. 2021.
[37] M. Sraitih and Y. Jabrane, "A denoising performance comparison based on ECG signal decomposition and local means filtering," *Biomed. Signal Process. Control*, vol. 69, Aug. 2021, Art. no. 102903.
[38] P. Singh and G. Pradhan, "Variational mode decomposition based ECG denoising using non-local means and wavelet domain filtering," *Australas. Phys. Eng. Sci. Med.*, vol. 41, no. 4, pp. 891–904, Dec. 2018.

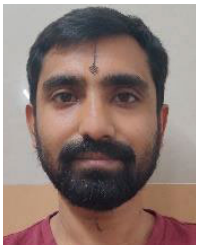

PAVAN G. MALGHAN received the B.E. degree in electronics and communication engineering from Visvesvaraya Technological University, Belgaum, Karnataka, India, in 2015, and the M.E. degree in signal processing from Savitribai Phule Pune University, Pune, Maharashtra, India, in 2017. He is currently pursuing the Ph.D. degree in ECG signal processing at the Vellore Institute of Technology, Vellore, Tamil Nadu, India. His research interests include digital signal and image processing, optimization algorithms, decomposition techniques, and denoising algorithms in biomedical applications.

MALAYA KUMAR HOTA received the M.Tech. degree in electronics engineering from the Visvesvaraya National Institute of Technology, Nagpur, India, in 2002, and the Ph.D. degree in electronics and communication engineering from the Motilal Nehru National Institute of Technology, Allahabad, India, in 2011. He is currently a Professor with the Department of Communication Engineering, School of Electronics Engineering, Vellore Institute of Technology, Vellore, Tamil Nadu, India. Previously, he was a Professor and a Principal with the Synergy Institute of Engineering and Technology, Dhenkanal, Odisha. He has more than 20 years of teaching and research experience. He has authored or coauthored about 35 publications. His research interests include digital signal processing, genomic signal processing, biomedical signal processing, seismic signal processing, and optimization techniques. He received one MODROBS grant from AICTE for the Modernization of Digital Signal Processing Lab. His biography has been included in Marquis Who's Who in Science and Engineering and also in Marquis Who's Who in the World.